

IMPROVING PRODUCT DESIGN BY PREDICTING FLEXURAL STRENGTH OF A HONEYCOMB CORE SANDWICH PANEL COMPOSITE USING PLY TENSILE STRENGTH

A Senior Project
presented to
the Faculty of the Materials Engineering Department
California Polytechnic State University, San Luis Obispo

In Partial Fulfillment
of the Requirements for the Degree
Bachelor of Science

by

Justin Lui
Javal Patel

June, 2015

© 2015 Justin Lui and Javal Patel

Abstract

The use of composite sandwich panels has increased in the aerospace industry. Prediction of a theoretical composite construction's flexural properties is important for efficient composite product designs. Utilizing the four point flexure geometry defined by Zodiac Aerospace, Santa Maria, CA, a mechanical model was derived to predict the flexural behavior of a theoretical honeycomb core sandwich composite using laminate tensile properties. The most common failure mode of Zodiac Aerospace's four point bend test is a failure in tension of the bottom laminate. Given this information, ASTM D3039 (Standard Test Method for Tensile Properties of Polymer Matrix Composite Materials) was chosen to test ply tensile properties. Based on the ASTM standard, a sample size of 30 specimens for each laminate was examined to account for any statistical variance. Specimen width was 1 inch, as suggested by the ASTM standard, and the thickness was 0.01 inches per ply on average. A high strength epoxy was used to adhere medium density fiberboard tabs to the fiberglass specimen to ensure failure occurred within the gage length. The tensile strength of a phenolic woven-fiberglass laminate construction with 1-ply, 2-ply, and 3-ply thicknesses was tested, inserted into the mechanical model, and compared to existing flexural data on sandwich panels tested by Zodiac Aerospace. The results indicate that the tensile strength increases as the number of plies are increased. The average tensile strength value for one, two and three ply are 38.8 ksi, 64.67 ksi and 71.22 ksi respectively. Although the flexural load of a sandwich panel with given dimensions was calculated using the ply tensile strength, the predicted loads may not be representative of the flexural loads measured in industry because the plies tested did not come from a population of batches, but from one batch.

Keywords: Honeycomb core sandwich panel, predict flexural load, four-point bending, tensile strength, tensile failure, delamination failure, materials engineering, composite materials, lamina properties, tensile testing composites, polymer matrix composites, fiberglass, 8-harness satin weave.

1	Table of Contents	
	Acknowledgments	iii
	List of Figures	iv
	List of Tables	iv
	Introduction	1
1.1	Composites Industry	1
1.2	Honeycomb Core Sandwich Panel Structure	3
1.3	Testing the Flexural Strength of a Sandwich Panel	5
1.4	Mechanics of Honeycomb Core Sandwich Panel Construction	
	Fracturing in Tension	7
2	Experimental Procedure	10
2.1	Safety Procedure	10
2.2	Tabbing Procedure	11
2.3	Instron Tensile Test Parameters	12
2.4	Statistics	13
3	Results	14
3.1	Tensile Test Results	14
3.2	Statistical Data	14
4	Analysis	17
4.1	Delamination vs. Tensile Failure	17
4.2	Tensile Strength Between 1-Ply, 2-Ply, and 3-Ply Facesheets	19
4.3	Flexural Load	21
5	Conclusions	22
	References	23
	Appendix A. Tensile Strength Data &for 1-, 2-, and 3-ply specimen	24
	Appendix B. Predicted Flexural Load of a 1-, 2-, and 3-ply tensile specimen	26

Acknowledgments

We would like to thank Professor Blair London for advising us through this project, Richard Morrison and Daniel Helms at Zodiac Aerospace for their continuous involvement with this project, and Zodiac Aerospace for sponsoring the project and providing committed support throughout the span of this project. We would also like to thank Lisa Rutherford for helping us with scheduling and the Materials Engineering department for providing the resources to conduct the necessary mechanical tests.

List of Figures

FIGURE 1. SCHEMATIC OF A HONEYCOMB CORE SANDWICH PANEL. THE LAYERS TYPICALLY INCLUDE A FACESHEET, ADHESIVE, AND A CORE.	2
FIGURE 2. MATERIALS COMPOSITION OF A 787 COMMERCIAL AIRLINER.	2
FIGURE 3. EXAMPLES OF VARIOUS APPLICATIONS OF HONEYCOMB CORE SANDWICH PANEL. (A) HELICOPTER SHELL. (B) BOEING 787 DREAMLINER WITH 20% HIGHER FUEL EFFICIENCY COMPARED TO 777.	3
FIGURE 4. SANDWICH CORE NOMENCLATURE, WHERE THE L-DIRECTION IS STRONGER AND W-DIRECTION IS WEAKER.	4
FIGURE 5. VISUAL REPRESENTATION OF AN 8-HARNESS SATIN WEAVE. THE WARP YARNS RUN VERTICALLY AND THE FILL YARNS RUN HORIZONTALLY.	5
FIGURE 6. TESTING SETUP FOR A THREE-POINT BEND TEST.	5
FIGURE 7. FOUR-POINT BEND TEST SETUP, WHERE THE SUPPORT SPAN LENGTH (S) AND LOADING SPAN (L), AND THE FORCE (P) MAY BE VARIED.	6
FIGURE 8. STRESS DISTRIBUTION OF A THREE-POINT BENDING TEST.	6
FIGURE 9. STRESS DISTRIBUTION OF A FOUR-POINT BENDING TEST.	7
FIGURE 10. DIMENSIONS OF THE CROSS-SECTION OF A HOLLOW RECTANGLE.	8
FIGURE 11. FREE BODY DIAGRAM OF THE SANDWICH PANEL. THE SUM OF THE MOMENT IS CALCULATED ABOUT THE SUPPORT.	9
FIGURE 12. INSTRON TENSILE TESTER ENCLOSED IN PLASTIC SHEETING AND COVERED WITH A PLASTIC SHIELD.	11
FIGURE 13. 40 POUND WEIGHTS WERE PLACED ON UP TO FIVE TENSILE SPECIMEN TO GET MAXIMUM ADHESION BETWEEN THE TAB AND PLY.	12
FIGURE 14. FINAL TABBED SPECIMEN.	12
FIGURE 15. DIMENSIONS OF THE TENSILE SPECIMEN. THE GRIP LENGTHS ARE TWO INCHES ON EACH SIDE OF THE SPECIMEN.	13
FIGURE 16. REPRESENTATIVE STRESS-STRAIN DIAGRAM WITH ALL THREE FACESHEET CONSTRUCTIONS. THERE ARE THREE GROUPINGS THAT ARE INDICATIVE OF THE PROPERTIES OF THE THREE PLY THICKNESSES.	14
FIGURE 17. BOX PLOT OF THE TENSILE STRENGTH FROM 1-PLY, 2-PLY, AND 3-PLY SAMPLES. THERE IS A GENERAL TREND OF INCREASING TENSILE STRENGTH AS MORE PLIES ARE BEING ADDED.	15
FIGURE 18. PREDICTED FLEXURAL LOAD OF A SANDWICH PANEL IN FOUR-POINT BENDING OF GIVEN DIMENSIONS USING THE TENSILE STRENGTH DATA MEASURED FROM INDIVIDUAL FACESHEET CONSTRUCTIONS.	17
FIGURE 19. A DIAGRAM OF THE HYPOTHESIZED TENSILE FAILURE ANGLE IS SHOWN.	18
FIGURE 20. AN EXTRAPOLATION OF THE TENSILE STRENGTH IS SHOWN. THE TENSILE STRENGTH OF THE FACESHEET WILL REACH AN ASYMPTOTE AS MORE PLIES ARE ADDED.	21

List of Tables

TABLE I. STATISTICAL DATA ON TENSILE STRENGTH FOR 1-PLY, 2-PLY, AND 3-PLY SAMPLES.	16
TABLE II. TUKEY PAIRWISE COMPARISON TEST ON DELAMINATION AND TENSILE FAILURE OF FACESHEETS .	19
TABLE III. AVERAGE PREDICTED MAXIMUM LOAD OF 1-PLY, 2-PLY, AND 3-PLY SAMPLES	20

Introduction

1.1 Composites Industry

A composite material is a combination of two materials that has properties that are not present in the two materials individually. Composites are used for applications that require lightweight and strong materials. A fiber-reinforced composite consists of a matrix and fibers bound together; the role of the matrix is to provide shape, as well as transfer the load to the fibers, which carries the entire load. The matrix is typically composed of a polymer, and the fiber can be composed of glass or carbon. The majority of composite materials used in the aerospace industry are fiber-reinforced composites, which have anisotropic mechanical properties.

The aviation industry uses sandwich-structured composites as an inexpensive method to increase the flexural strength of fiber-reinforced composites by increasing the second moment of inertia of the structure. The core of the sandwich panel does not need to be strong because it does not carry the load, so an inexpensive material is usually used. The most important quality of the core is its ability to bond with the facesheets in order to transfer loads between the top and bottom facesheets. A honeycomb core sandwich panel is lighter due to the hollow space in the core, and therefore it is highly popular in the aerospace industry (**Figure 1**)¹. The disadvantage of using composite materials is the high cost due to the difficulty of manufacturing.

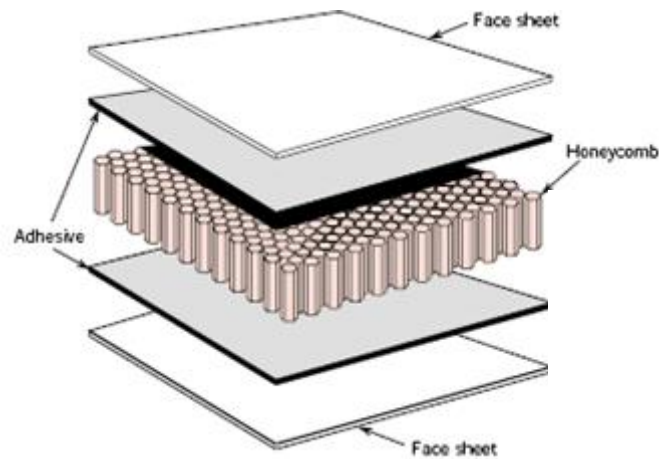


Figure 1. Schematic of a honeycomb core sandwich panel. The layers typically include a facesheet, adhesive, and a core.

Although the initial cost of manufacturing composites is high, airline companies still want to use composite materials because the reduced weight will save fuel over the whole life of the jet. In fact, composites make up a large portion of the exterior of a commercial jetliner; 50% of the 787 jet is composed of either a carbon laminate or a carbon sandwich composite (**Figure 2**)².

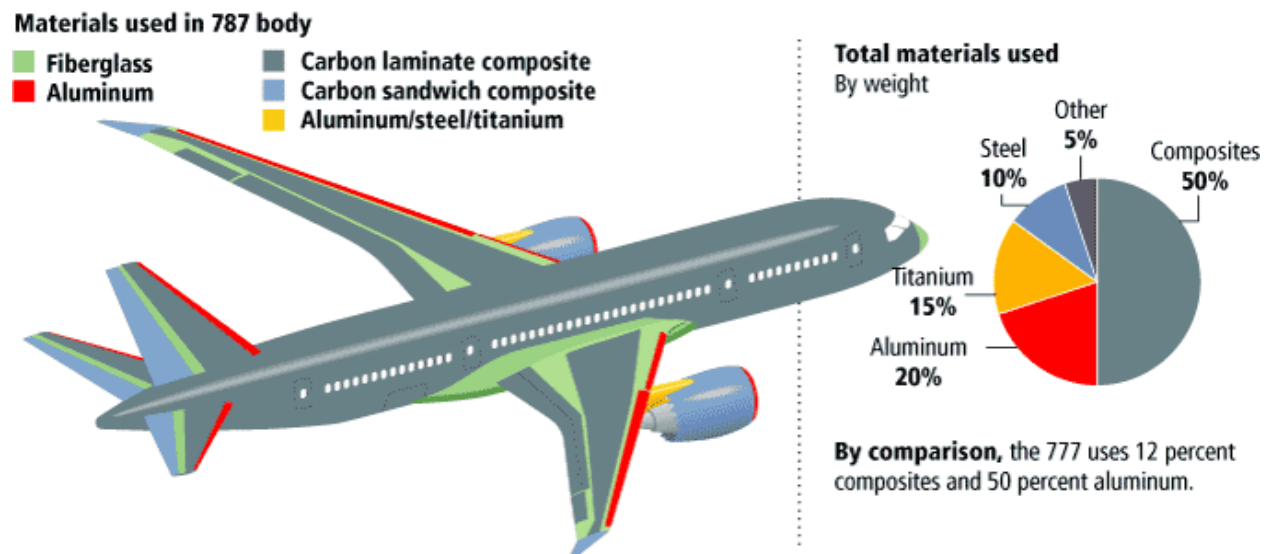


Figure 2. Materials composition of a 787 commercial airliner.

Sandwich structures can be found in Navy applications such as deep ocean vessels, minesweepers, and helicopter shell. Over 80% of Boeing's Dreamliner contains composite material (**Figure 3**)^{3,4}. The cylindrical fuselage shell in the Boeing 747 is primarily made from a Nomex® honeycomb sandwich construction, along with the floors, side panels, overhead bins and ceiling.

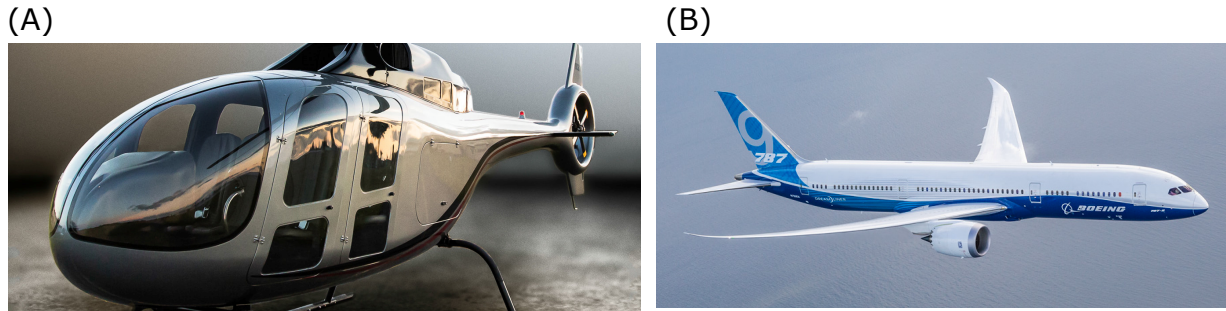


Figure 3. Examples of various applications of honeycomb core sandwich panel. (A) Helicopter shell. (B) Boeing 787 Dreamliner with 20% higher fuel efficiency compared to 777.

Zodiac Aerospace is a French company that produces and develops aerospace equipment and systems. There are five major divisions at Zodiac Aerospace including: Aircraft Systems, AeroSafety, Gallery & Equipment, Cabin & Structures, and Seats. During the year 2013-2014, Zodiac Aerospace had a gross revenue of €4.17 billion and a net income of €354 million.⁵

This senior project focuses on the Zodiac Aerospace Cabin & Structures division, which mainly uses honeycomb composite sandwich panels to make interior parts of private jet planes.

1.2 Honeycomb Core Sandwich Panel Structure

The honeycomb core contains W and L directions. The W-direction runs parallel to the adhesive that bonds the core. Therefore the W-direction is the weaker direction when pulled along the L-direction because the adhesive is weaker than the primary bonds of the paper (**Figure 4**). On the other hand, pulling in the L-direction is strong because the core's Young's modulus is significantly greater than the adhesive strength. Therefore, both the core and the facesheets are anisotropic –

the property of the sandwich panel will be dependent on both the core and facesheet orientation.

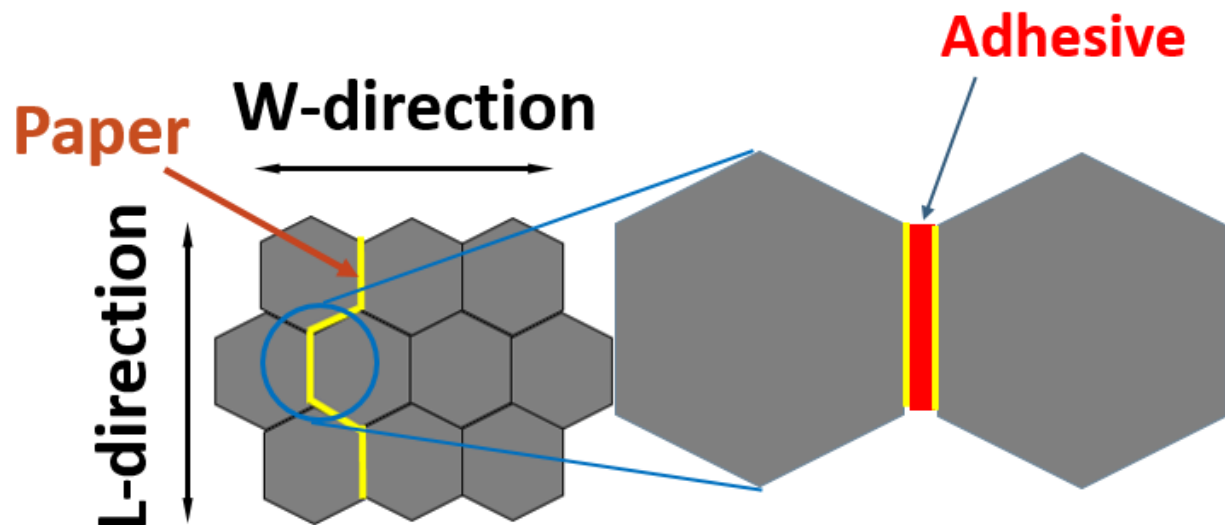


Figure 4. Sandwich core nomenclature, where the L-direction is stronger and W-direction is weaker.

The plies of the sandwich panel at Zodiac Aerospace Cabin & Structures are composed of glass fibers in an 8-harness satin weave and the matrix used is a phenolic-based resin. A weave is composed of two classifications of yarn – a warp yarn and a fill yarn. The warp yarn runs lengthwise along the direction of the roll and is continuous for the entire length. The fill yarn is the tow that is 90° to the roll direction and runs along the width. In an 8-harness satin weave, the fill yarn floats over seven warp yarns and under one (**Figure 5**)⁶. This type of weave is the most pliable weave used in industry and forms well around compound curves. The strength of the weave is stronger in the warp direction than in the fill direction. The reason behind this is because during manufacturing of the weave, the warp fibers are pulled in tension while the fill fibers are woven. Therefore, warp fibers are more aligned and taught than fill fibers throughout the facesheet.

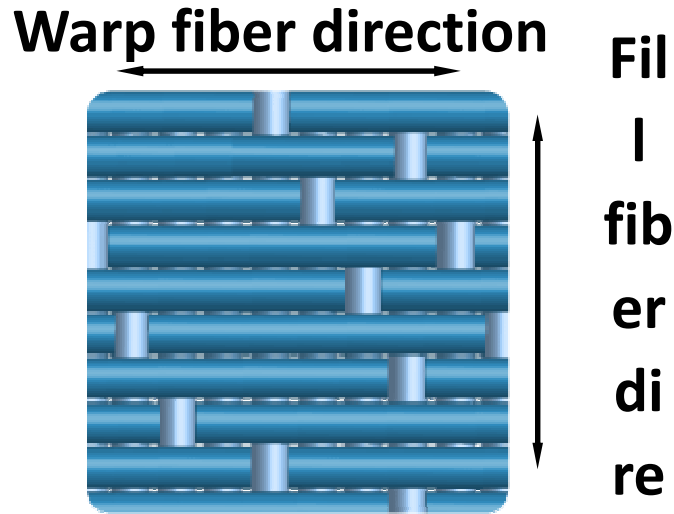


Figure 5. Visual representation of an 8-harness satin weave. The warp yarns run vertically and the fill yarns run horizontally.

1.3 Testing the Flexural Strength of a Sandwich Panel

The flexural strength of a material describes its ability to resist bending under a certain load. The two main tests to experimentally determine the flexural strength are a three-point bend test and a four-point bend test. In a three-point bend test, there are two supports holding the specimen and one load point in the center of the specimen (**Figure 6**)⁷.

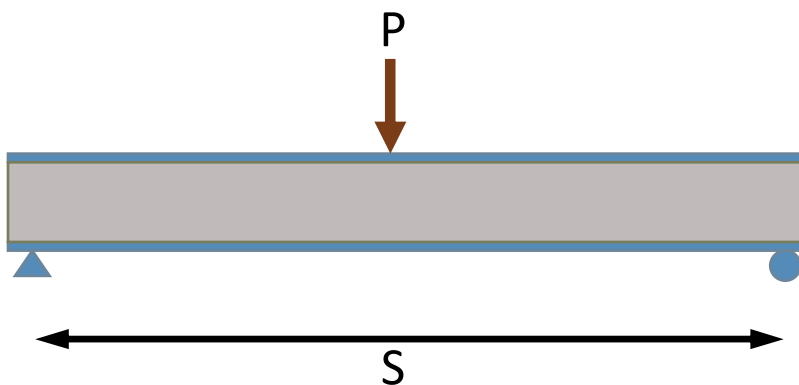


Figure 6. Testing setup for a three-point bend test.

In a four-point bend test, there is a similar support span holding the specimen but now two load points that are equally spaced from the center of the sample producing the loading span (**Figure 7**).

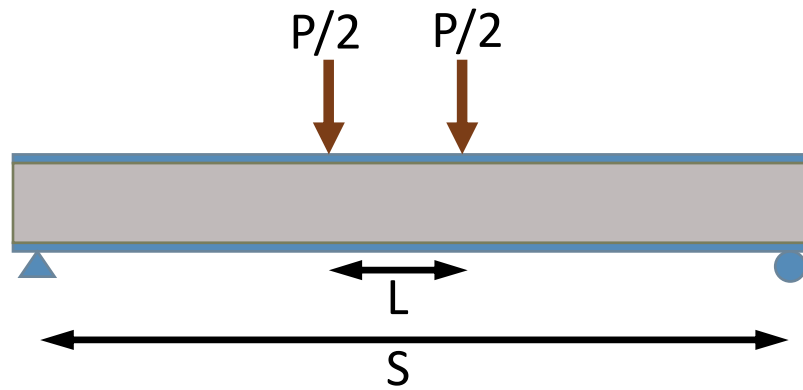


Figure 7. Four-point bend test setup, where the support span length (S) and loading span (L), and the force (P) may be varied.

The main difference between the three-point and four-point bend tests is the stress distribution across the facesheets. In a three-point bend test, the maximum stress is located immediately under the loading nose (**Figure 8**).

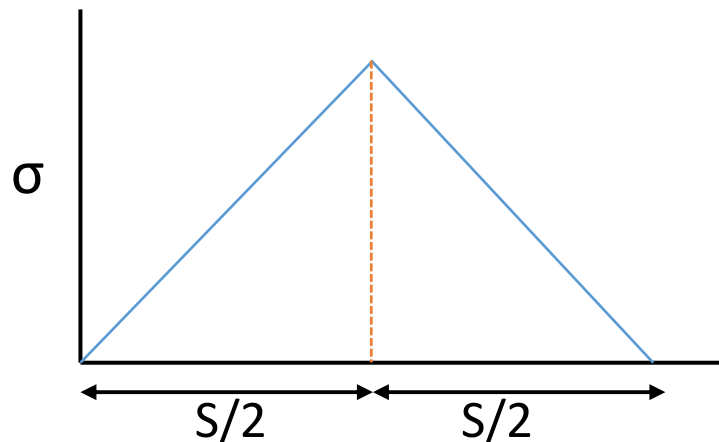


Figure 8. Stress distribution of a three-point bending test.

On the other hand, in a four-point bend test, the maximum stress is distributed evenly between the loading noses (**Figure 9**).⁸ Determining which type of test to use depends on the application of the specimen.

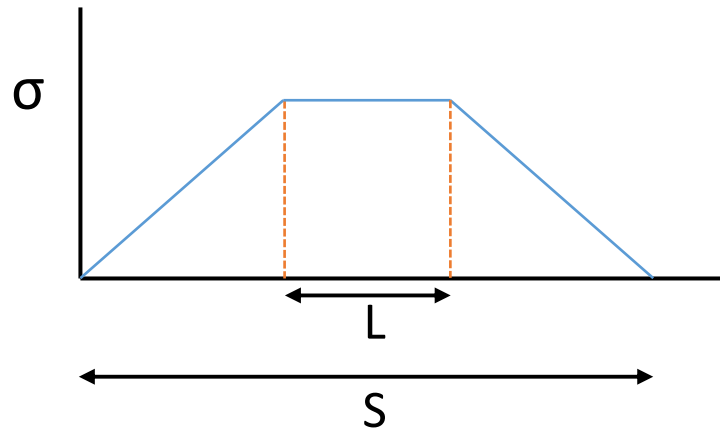


Figure 9. Stress distribution of a four-point bending test.

1.4 Mechanics of Honeycomb Core Sandwich Panel Construction

Fracturing in Tension

The failure of a sandwich panel composite under bending can fail in multiple ways. A few of the failure mechanisms are compressive facesheet failure, facesheet debonding, indentation failure, core failure, and compression face wrinkling. Different failure modes can occur during testing based on the components of the sandwich panel, geometry of the panel, and testing method. To predict the flexural strength of a sandwich panel, the most prominent failure mechanism must be known, as it will determine the mechanical details behind the prediction. In some cases, properties of the core or the interaction between the core and facesheets may need to be characterized to make an accurate prediction of the flexural strength.

Zodiac Aerospace conducts a four point bend test of the sandwich panel, which is a modified ASTM D7249 test. In this test, a majority of their honeycomb sandwich panel composites fail in tension of the bottom ply under four-point loading. As a

result, the material properties of the core are not considered in the prediction of flexural strength in a honeycomb sandwich panel composite. The stiffness of the core is assumed to be negligible because the stiffness of the core is much less than the stiffness of the facesheets. The influence of the core is negligible until its stiffness is 1/200 times the facesheet modulus.⁹ Therefore, the core acts as a void space that increases the second moment of inertia. The tensile properties of the facesheet are of interest to predict the flexural strength of the sandwich panel.

An equation that related the ultimate tensile stress of a ply to the flexural strength of a honeycomb core sandwich panel was derived using the bending stress under simple bending (**Eq. 1**).

$$\sigma = \frac{M}{I} y \quad (\text{Eq. 1})$$

Where M is the bending moment about the neutral axis, y is the perpendicular distance to the neutral axis, and I is the second moment of area about the neutral x -axis. The second moment of area is the geometrical property of an area, which reflects how its points are distributed with regard to an arbitrary axis.

For a honeycomb core sandwich panel, the second moment of area would resemble a cross-sectional area similar to a hollow rectangle (**Figure 10**).

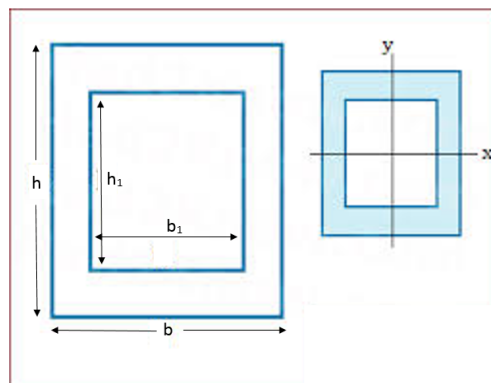


Figure 10. Dimensions of the cross-section of a hollow rectangle.

The equation for the second moment of area of a hollow rectangle is given by (**Eq. 2**).

$$I_x = \frac{1}{12} [bh^3 - b_1h_1^3] \quad (\text{Eq. 2})$$

In a sandwich panel, b_1 is equal to b because there is no facesheet material on the sides of the panel. The relationship between h and h_1 is the total height of the panel subtracted by twice the thickness of the facesheet (h_f) (**Eq. 3**).

$$h_1 = h - 2h_f \quad (\text{Eq. 3})$$

The thickness of the facesheet is directly related to the number of plies. Therefore, the equation relating facesheet thickness to number of plies is given by $h_f = t_p * n$, where t_p is the thickness of one ply, and n is the number of plies.

To solve for M in Eq.1, the distance between the supports and loading noses must be known. A four-point bending test setup is shown in Figure 7.

To solve for M , the sum of the moments was set to zero about the support (**Figure 11**).

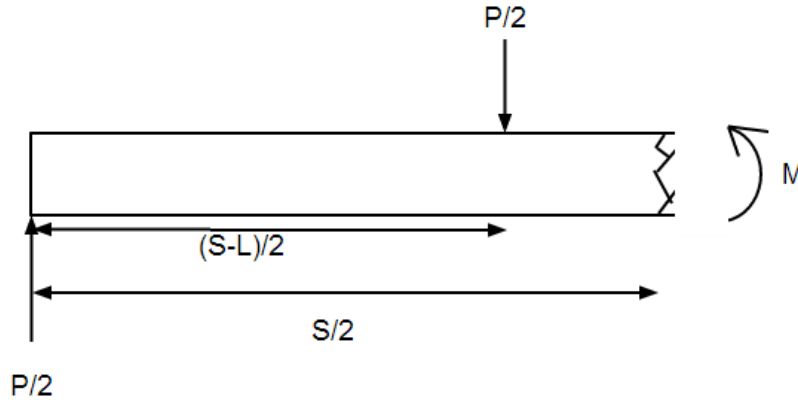


Figure 11. Free body diagram of the sandwich panel. The sum of the moment is calculated about the support.

The moment can be calculated using the geometry of the specimen and testing setup (**Eq. 4**).

$$M = \frac{P}{2} [S - L] \quad (\text{Eq. 4})$$

Combining Eq. 1, Eq. 2, Eq. 3, and Eq. 4, the general equation for the flexural strength of a sandwich panel composite is given by **(Eq. 5)**.

$$\sigma = \frac{3Ph[S - L]}{b[h^3 - (h - (2t_p * n))^3]} \quad \textbf{(Eq. 5)}$$

Because σ is a material property of the ply, the value should theoretically remain constant. Therefore, the equation was solved for P **(Eq. 6)**.

$$P = \frac{\sigma b[h^3 - (h - (2t_p * n))^3]}{3h[S - L]} \quad \textbf{(Eq. 6)}$$

To find the flexural strength of Zodiac Aerospace panels, the dimensions of their test fixtures and specimen must be known in order to get an accurate prediction using ply tensile strength.

2 Experimental Procedure

To conduct a tensile test on the facesheet, ASTM D3039 (Standard Test Method for Tensile Properties of Polymer Matrix Composite Materials) was used to measure the tensile strength. A total of 90 specimens were tested, with 30 for each 1-, 2- and 3-ply specimens. The failures of the majority of plies were video recorded for reference to explain any outlying data.

2.1 Safety Procedure

To ensure proper safety during testing, a fiberglass respiratory mask and safety goggles that covered the sides of the eyes were worn. Additionally, the Instron tensile test machine was enclosed with plastic sheeting so fibers could not escape into the testing room **(Figure 12)**. It was also made sure that no one else entered the lab during testing.



Figure 12. Instron tensile testing machine enclosed with a plastic shield.

2.2 Tabbing Procedure

To prevent grip failure, medium density fiberboard (MDF) tabs were cut out and the surfaces were roughened with emery paper for better adhesion between the tab and the epoxy. Loctite 9340 Hysol[®] was used as the epoxy to bond the tabs to the composite specimen. The shear strength of this particular epoxy is 2300 psi at a room temperature of 77°F so it would provide sufficient strength to prevent slipping of the tabs during testing.¹⁰ This epoxy adhesive paste has two parts that were mixed in a 1:1 ratio and cured for 72 hours at room temperature.

To remove any organics on the specimens and tabs, acetone was used to clean the surface of any organics thoroughly. After air drying the specimens, the epoxy was applied to the tabs and cured for 72 hours under 40 lbs. of steel blocks to ensure maximum adhesion between the tabs and ply (**Figure 13**). If tabs were not completely in contact with the ply, then stress concentrations from the grips may induce premature failure of the testing specimen.

The resulting tabbed specimen look like the samples shown in **Figure 14**.



Figure 13. 40 pound weights were placed on up to five tensile specimen to get maximum adhesion between the tab and ply.

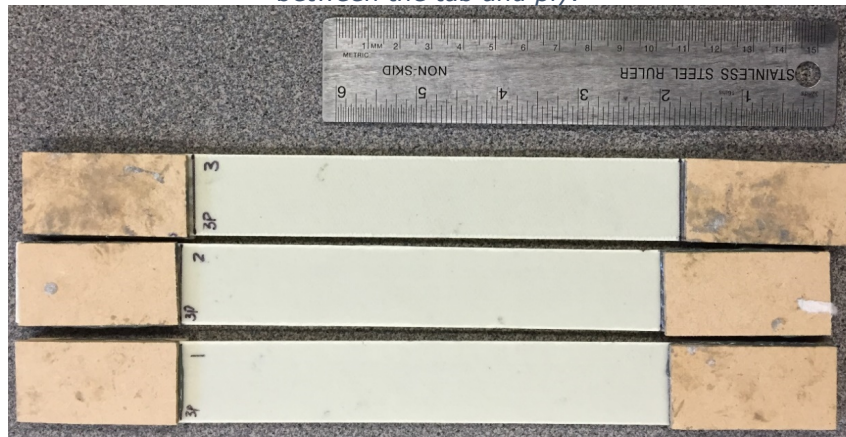


Figure 14. Final tabbed specimen

Batches of five 1-ply, 2-ply, and 3-ply samples were made at a time. This minimizes the impact of throwing out samples if there were any mistakes when tabbing the specimens.

2.3 Instron Tensile Test Parameters

After the samples were prepared, an Instron 150kN capacity testing system was used to conduct the tensile tests. For the testing parameters, a cross head displacement rate of 0.05 inches per minute was used. The sample dimensions were 10 inches in length and 1 inch in width, with a gage length of 6 inches (**Figure 15**). The thickness of each specimen depended on the number of plies that each facesheet was composed of. The dimensions of each sample were measured using digital calipers accurate to ± 0.001 inches and input into the Instron software to accurately measure the tensile properties of each ply.

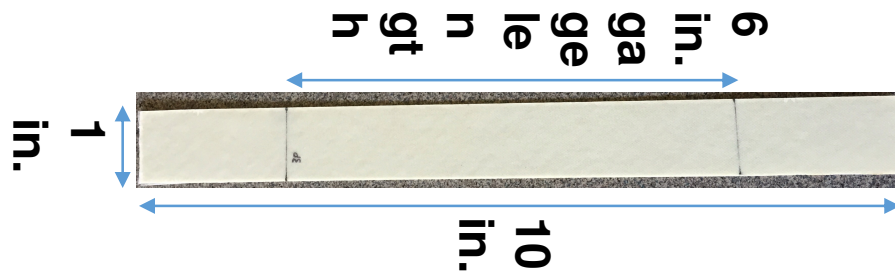


Figure 15. Dimensions of the tensile specimen. The grip lengths are two inches on each side of the specimen.

Tensile tests were completed until fracture or failure of the ply specimens. Since the tensile strength was the property that was of interest, no extensometer was used to accurately measure strain. Therefore, the measured strain is from cross-head displacement.

A mix of facesheet thicknesses were tested during a given testing timeframe to minimize the impact of recording wrong data if testing was not done correctly (i.e. recording 9 bad values for 1-ply vs. 3 bad values for 1-, 2-, and 3-ply samples).

2.4 Statistics

An analysis of variance test (ANOVA) and Tukey pairwise comparison test were applied on the measured tensile strength data in order to compare if the values were significantly different from each other.

In addition, two failure modes were observed when testing the specimen. One type was a tensile failure, and the other was delamination. An ANOVA and Tukey test

were also applied to test if the tensile strengths were significantly different for specimen failing in delamination and tension.

3 Results

3.1 Tensile Test Results

After conducting the tensile tests, a series of stress-strain curves as well as tables for the ply tensile property values were produced. A representative stress-strain curve is shown in **Figure 16**.

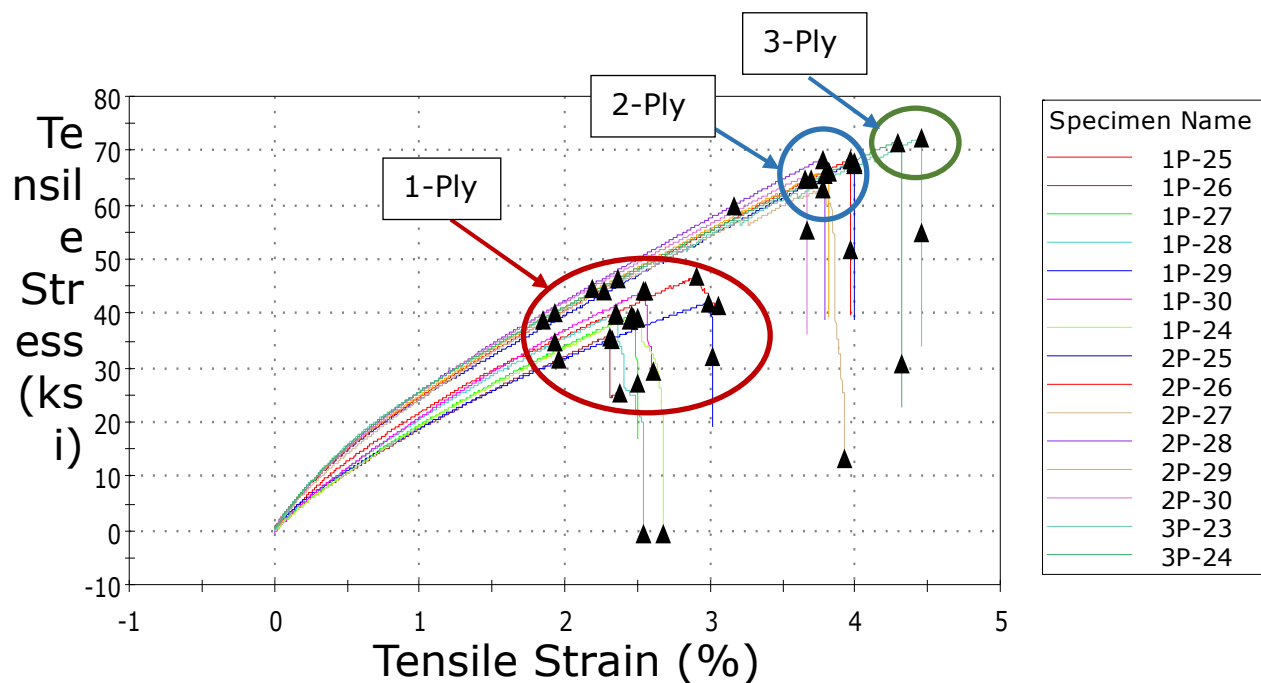


Figure 16. Representative stress-strain diagram with all three facesheet constructions. There are three groupings that are indicative of the properties of the three ply thicknesses.

3.2 Statistical Data on Tensile Strength and Failure Mode

Raw tensile strength values for thirty of each facesheet construction were input into Minitab to apply statistical testing. A box plot was produced to get a better visualization of the tensile strength of the facesheet constructions (**Figure 17**).

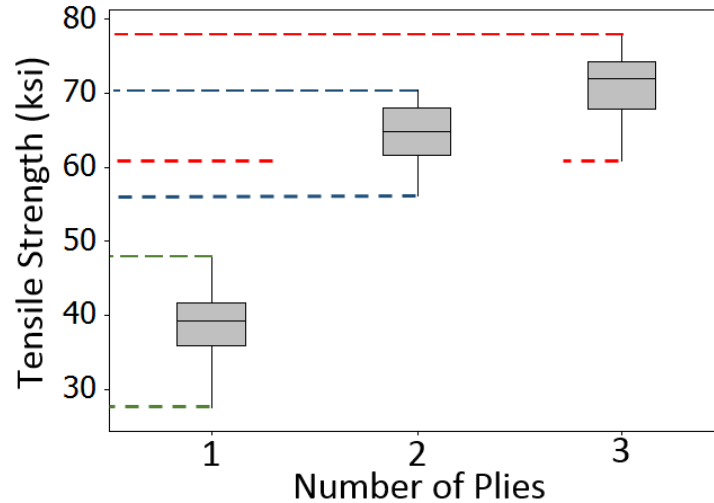


Figure 17. Box plot of the tensile strength from 1-ply, 2-ply, and 3-ply samples. There is a general trend of increasing tensile strength as more plies are being added.

When observing the failures of the test specimens, five out of thirty samples failed in delamination for 2-ply samples. Ten out of thirty samples failed in delamination for 3-ply samples (**Figure 18**).

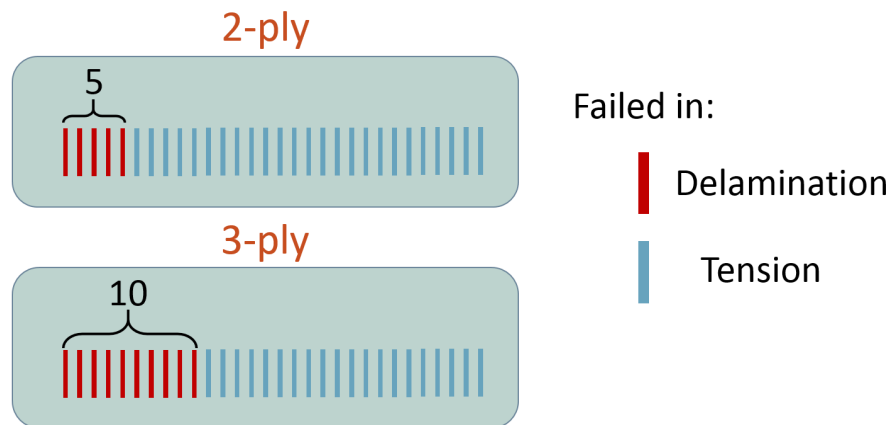


Figure 18. Distribution of failure modes seen in 2-ply and 3-ply samples.

ANOVA and Tukey pairwise comparison tests were applied to the tensile strengths of specimen failing in delamination and tension to determine if the values are significantly different from each other (**Table I** & **Table II**). If the tensile strengths were significantly different, then the data for delaminated specimens would have to

be removed from the total dataset because the failure mode does not correspond to that of Zodiac's sandwich panel.

Table I. Tukey Comparison Test between 2-Ply Specimen That Failed in Delamination and Tension

2-Ply	# of Samples	Mean (TS)	Grouping
Delamination	5	65.99	A
Tension	25	64.40	A

Table II. Tukey Comparison Test between 3-Ply Specimen That Failed in Delamination and Tension

3-Ply	# of Samples	Mean (TS)	Grouping
Delamination	10	72.15	A
Tension	20	70.76	A

The p-value that was returned was <0.0001 and the Tukey pairwise comparison test indicated that the different failures did not yield a significantly different tensile strengths. Therefore, we were able to include both failure modes in the overall dataset for tensile strength of the facesheets. Having more tensile strength values will strengthen the statistical analysis when comparing 1-ply, 2-ply, and 3-ply specimen.

Tables of the tensile strengths, maximum load, and accompanying dimensions of 1-ply, 2-ply, and 3-ply samples can be found in **Appendix A**. Statistical data on all three facesheet constructions are listed (**Table III**).

Table III. Statistical Data on Tensile Strength for 1-Ply, 2-Ply, and 3-Ply Samples

	1-ply	2-ply	3-ply
Average Tensile Strength (ksi)	38.80	64.67	71.91
Standard Deviation (ksi)	4.54	3.64	3.69
Range (ksi)	20.79	14.55	12.63

A predicted flexural load was produced by inserting the tensile strength data into σ term in Eq. 6. According to Zodiac's four-point bending tests for this particular sandwich panel, the dimensions for the sandwich panel and four-point bending loading setup were $b = 3 \text{ in.}$, $h_c = 0.5 \text{ in.}$, $h = h_c + (2 * \text{ply thickness})$, $S = 22 \text{ in.}$, and $L = 4 \text{ in.}$. The raw flexural strength values are listed in **Appendix B**. A boxplot of the predicted flexural load is shown in **Figure 19**.

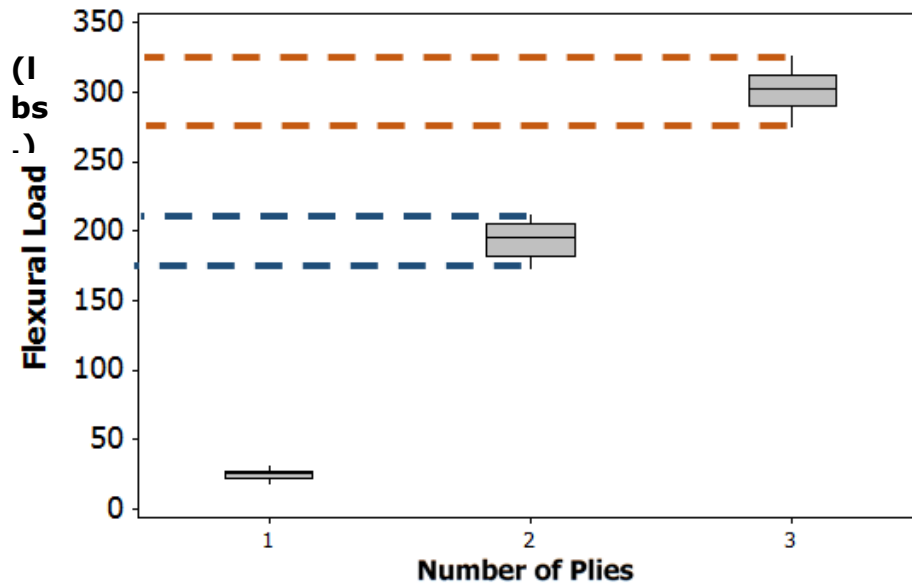


Figure 19. Predicted flexural load of a sandwich panel in four-point bending of given dimensions using the tensile strength data measured from individual facesheet constructions.

4 Analysis

4.1 Delamination vs. Tensile Failure

Both tensile failure and delamination failures were observed when tensile testing the plies. Tensile failure occurs due to defects on the sample, causing stress concentrations where leading to a stress concentration at a specific point where the fiber is more likely to fail. Defects are inherent in a glass fiber, but additional defects can be added throughout the manufacturing process.

During tensile failure, the ply acts like a cloth, tearing diagonally instead of horizontally. A possible explanation to this mode of failure is due to the way an 8-harness weave is structured. As the specimen fails, the angle of the failure is close

to the angle formed where the fill fiber intersects a warp fiber. At the intersection, fiber undulation is present which may lead to local stresses at the fiber interface, leading to preferential failure at that location (**Figure 20**).

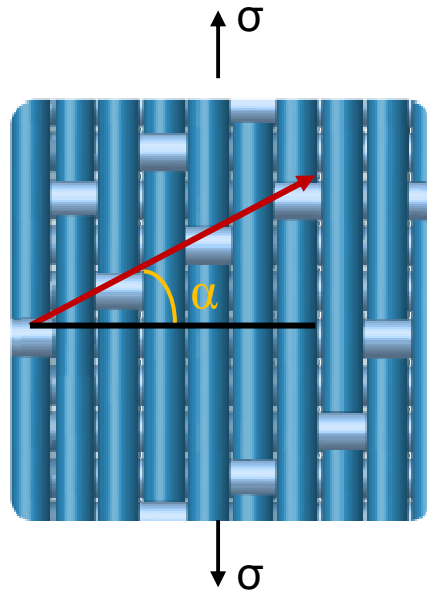


Figure 20. Hypothesized tensile failure angle is based off of the angle between the warp fibers and weave of the fill fibers.

Delamination failure was observed in a sixth of the specimens for 2-ply and a third of the specimens for 3-ply facesheets. The hypothesis for this mode of failure was that the fibers resisted failure before the load overcame the shear strength between the plies, leading to delamination. In delamination failure, the mode of failure was gradual because of the way the plies are bonded together; the ply failed in steps as more of the ply delaminated. To explain why delamination could occur, the manufacturing of the facesheet has to be understood. During the manufacturing process, the plies were compressed at high pressure and temperature. As a result, the processes "melts" the resin together therefore leading to a strong bond between the resin of both the plies. In addition, the manufacturing method of cutting the facesheets partially delaminated some of the specimens, leading to a slightly preferential delamination failure during the tensile test.

To determine if the tensile strength of delamination failures could be included in the total dataset, an ANOVA test and Tukey pairwise comparison test were applied to

test if there was a significant difference between the two failure modes. The p-value that was returned was <0.0001 and the Tukey pairwise comparison test indicated that the different failures did not yield a significantly different tensile strengths (**Table IV**).

Table IV. Tukey Pairwise Comparison Test on Delamination and Tensile Failure of Facesheets

	Grouping		
1-Ply	A		
2-Ply		B	
3-Ply			C

By proving that the tensile strengths of delamination and tensile failures were not significantly different, the data from both failures can be used in the total data set. Not having to remove tensile strength values from the dataset would strengthen the statistical analysis when comparing 1-ply, 2-ply, and 3-ply specimen.

4.2 Tensile Strength between 1-Ply, 2-Ply, and 3-Ply Facesheets

The average tensile strength from 1-ply to 2-ply increased 67% whereas from 2-ply to 3-ply there was only 11% increase (**Table III**). To test if the tensile strengths of the facesheets were significantly different, an ANOVA test and Tukey pairwise comparison test was conducted on the tensile strengths. A p-value of <0.0001 was returned and the Tukey test concluded that the tensile strengths between the three facesheets were all significantly different from each other.

The initial increase from one to two ply can be explained by the shear forces acting between the plies that adds to the overall load, which in turn increases the tensile strength. As the number of plies increases, there is a higher fiber-to-resin ratio due to the compressive forces squeezing the resin out during manufacturing. Therefore,

the total thickness of the facesheets is not proportional as plies are added. This could also be the reason why the tensile strength is not constant as the ply thickness increases, as is seen in other materials such as metals and plastics.

The tensile strength increase between 2-ply and 3-ply facesheets is moderate because the shear force between plies is present in both constructions. Adding plies also increases the number of defects in the ply where failure can originate. Despite this fact, the tensile strengths were inserted into the σ term in (Eq. 6). The predicted load at which the facesheets failed was higher as more plies were added (**Table V**).

Table V. Average predicted maximum load of 1-ply, 2-ply, and 3-ply samples

	1-Ply	2-Ply	3-Ply
Average Maximum Load (lbs.)	73.71	193.91	299.58

The stress-strain curve of the tensile test depicts that the failure for the plies is instantaneous when it reaches the maximum tensile strength (Figure 16). Unlike metals, there is no necking because the majority of the load is carried by the fibers. Therefore, there comes a point when the load applied exceeds the maximum load the fibers are able to withstand. It can also be noted that there is an overlap between some of the tensile strength values for 2- and 3-ply facesheets but no overlap for 1- and 2-ply specimens. The overlap between two and three plies suggests that adding additional plies will not lead to a major increases in the tensile strength of the specimen.

An extrapolation of the tensile strength based on 1-ply, 2-ply, and 3-ply tensile data was plotted. The predicted tensile strength of a 4-ply facesheet is also plotted based on its thickness. From the graph, the tensile strength will eventually reach an asymptote if the number of plies was continually increased (**Figure 21**).

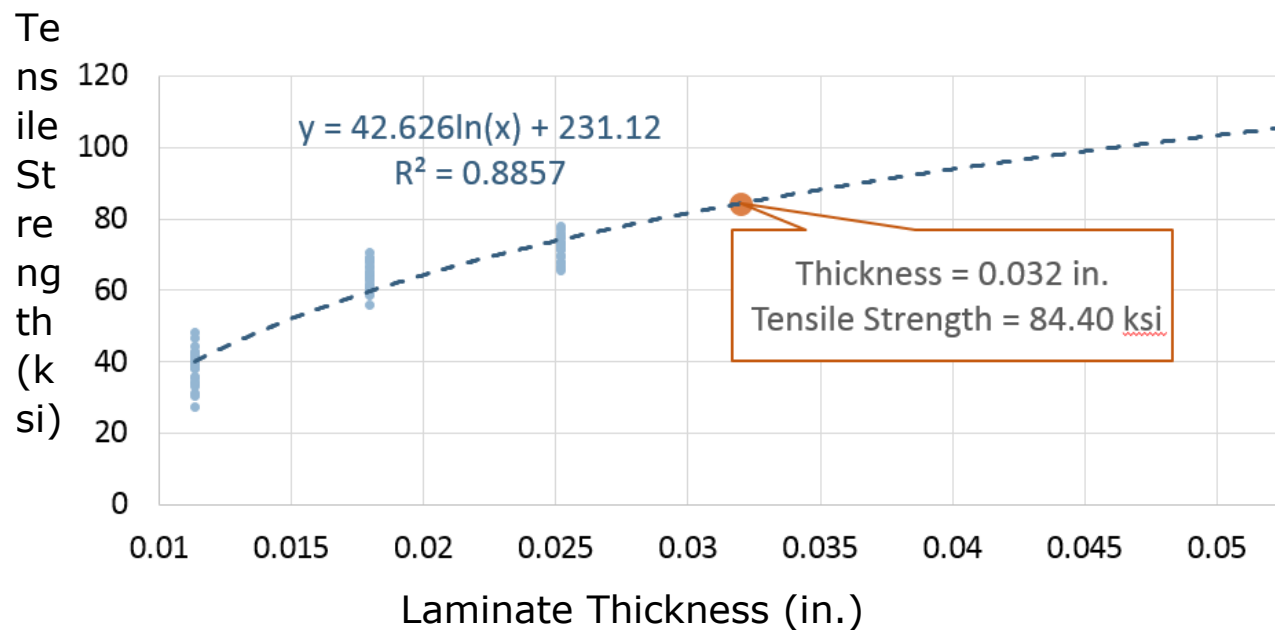


Figure 21. An extrapolation of the tensile strength. The tensile strength of the facesheet will reach an asymptote as more plies are added.

4.3 Flexural Load

There is a chance that the predicted flexural load of the sandwich panel construction may not be representative of the industry tested values because of the sample population of the tensile test. Predicted flexural load of 1-, 2- and 3-ply can be found in **Appendix B**. All specimens tested were taken from the same batch for each thickness of facesheets. Therefore, the tensile tests conducted on the plies only represented the variance within one batch, not the variance between a whole population of batches. The composite industry values for flexural load will be B-basis values, which take into account many batches of facesheets. In addition, since the facesheets were provided, the manufacturing of the plies is not 100% certain. Therefore, the orientation of the plies within a facesheet could vary between ply thicknesses. For example, the 2-ply specimen could be $0^\circ, 90^\circ$ whereas the 3-ply specimen could be $0^\circ, 0^\circ, 0^\circ$. A change in ply orientation would significantly change the tensile properties of the facesheet. This would dramatically affect the tensile strength values measured, since the tensile strength of the warp fiber direction is much stronger than that of the fill direction.

Despite the reasons why the predicted flexural load could be different than the experimentally tested sandwich panel flexural loads, the two values were compared. Only experimental values for 2-ply tensile strengths with differing core heights were received. The % difference between the predicted and experimental flexural loads were low.

5 Conclusions

1. The percent difference between the predicted flexural load and the experimental flexural load was low.
2. The tensile strength of 1-, 2-, and 3-ply are significantly different from each other. The average tensile strength values are 38.8 ksi, 64.67 ksi and 71.22 ksi respectively.
3. The predicted flexural load calculated from the ply tensile strength may not be representative of the actual flexural load in industry.
4. There is no significant difference between the tensile strength of delamination and tensile failure within the same laminate construction.

References

- 1 Jaafar, Fariezul. "Sandwich Composite and Core Material." *Fiber Reinforced Plastic*. The Fibre Reinforced Plastic & Composite Technology Resource Centre, 12 Dec. 2010. Web. 26 Jan. 2015.
- 2 "Boeing 787/7E7 Dreamliner." Web log post. *Boeing 787 Dreamliner-Specs*. N.p., n.d. Web. 26 Jan. 2015. <http://modernairliners.com/Boeing787_files/Specifications.html>.
- 3 "787 Dreamliner Airplane | Boeing Commercial Airplanes." *Boeing's New Airplane*. The Boeing Company, n.d. Web. 27 Jan. 2015.
- 4 *Composite Helicopters*. Composite Helicopters International, n.d. Web. 27 Jan. 2015.
- 5 Zodiac Aerospace 2013/2014 *Annual Report*, 2014. Web. 25 Jan 2015.
- 6 "Woven Fabric Style Guide." ACP Composites Woven Fabric Selection Guide. ACP Composites Inc., n.d. Web. 02 Nov. 2014.
- 7 Kopeliovich, Dmitri. "Materials Engineering." *Flexural Strength Tests of Ceramics*. SubsTech, 1 June 2012. Web. 27 Jan. 2015.
- 8 ASTM Standard D7264, 2007, "Standard Test Method for Flexural Properties of Polymer Matrix Composite Materials", ASTM International, West Conshohocken, PA, 2007, 10.1520/D7264_D7264M-07
- 9 Isaac M Daniel, Jandro L Abot, Fabrication, testing and analysis of composite sandwich beams, *Composites Science and Technology*, Volume 60, Issues 12-13, September 2000, Pages 2455-2463, ISSN 0266-3538
- 10 "Product Description Sheet - Hysol® Product 9340." Scottsales. Loctite, Aug. 2001. Web. Mar. 2015. <[http://www.scottsales.com/Epox i-Patch-Kits/HysA9340-EN.pdf](http://www.scottsales.com/Epox%20i-Patch-Kits/HysA9340-EN.pdf)>.

Appendix A: Tensile Strength Data &for 1-, 2-, and 3-ply specimen

1-ply data generated from tensile test

1 Ply	TS (ksi)	Maximum Load (kips)	Thickness (in.)	Width (in.)
1P,1	37.42	0.45	0.012	1.006
1P,2	41.51	0.5	0.012	1.011
1P,3	39.09	0.47	0.012	1.005
1P,4	38.02	0.46	0.012	1.0015
1P,5	42.49	0.47	0.011	1.005
1P,6	41.34	0.5	0.012	1.006
1P,7	38.35	0.43	0.011	1.0095
1P,8	39.07	0.43	0.011	1.005
1P,9	35.57	0.43	0.012	1.009
1P,10	48.21	0.48	0.012	1.004
1P,11	42.02	0.51	0.012	1.005
1P,12	42.83	0.43	0.012	1.01
1P,13	38.72	0.43	0.011	1.004
1P,14	40.42	0.41	0.012	1.007
1P,15	41.53	0.46	0.011	1.005
1P,16	31.07	0.34	0.011	1.008
1P,17	30.3	0.33	0.011	0.997
1P,18	33.24	0.37	0.011	1.004
1P,19	34.06	0.38	0.011	1.002
1P,20	27.42	0.3	0.011	1
1P,21	38.71	0.43	0.011	1.007
1P,22	34.23	0.38	0.01	1.008
1P,23	40.29	0.4	0.01	1.007
1P,24	39.38	0.48	0.012	1.008
1P,25	46.76	0.52	0.011	1.005
1P,26	35.85	0.4	0.011	1.003
1P,27	39.93	0.48	0.012	1.007
1P,28	39.93	0.44	0.011	1.011
1P,29	42.12	0.51	0.012	1.003
1P,30	44.21	0.49	0.011	1.006

2-ply data generated from tensile test

2 Ply	TS (ksi)	Maximum Load (kips)	Thickness (in.)	Width (in.)
2P,1	69.59	1.26	0.018	1.0015
2P,2	62.73	1.13	0.018	1.009
2P,3	69.82	1.26	0.018	1.009
2P,4	66.45	1.20	0.018	1.005
2P,5	64.75	1.17	0.018	1.007
2P,6	62.99	1.21	0.019	1.004

2P,7	67.85	1.23	0.018	1.01
2P,8	69.22	1.26	0.018	1.013
2P,9	68.94	1.18	0.017	1.007
2P,10†	65.11	1.12	0.017	1.01
2P,11	64.84	1.24	0.019	1.007
2P,12†	66.9	1.21	0.018	1.0035
2P,13†	70.54	1.28	0.018	1.0055
2P,14†	64.59	1.23	0.019	1.006
2P,15	55.99	1.07	0.019	1.009
2P,16	63.4	1.09	0.017	1.003
2P,17	58.82	1.07	0.018	1.007
2P,18	63.62	1.09	0.017	1.004
2P,19	60.56	1.04	0.017	1.006
2P,20	60.64	1.1	0.018	1.008
2P,21	60.66	1.1	0.018	1.008
2P,22	59.97	1.08	0.018	1.003
2P,23	61.46	1.11	0.018	1.003
2P,24	61.62	1.12	0.018	1.007
2P,25	67.87	1.23	0.018	1.0025
2P,26	68.44	1.24	0.018	1.007
2P,27†	62.85	1.14	0.018	1.005
2P,28	68.58	1.24	0.018	1.008
2P,29	66.3	1.2	0.018	1.007
2P,30	64.98	1.18	0.018	1.005

† Specimen that failed in delamination

3-ply data generated from tensile test

3 Ply	TS (ksi)	Maximum Load (kips)	Thickness (in.)	Width (in.)
3P,1	73.43	1.91	0.025	1.008
3P,2	72.15	1.88	0.026	0.9935
3P,3	69.21	1.8	0.026	1.007
3P,4	65.75	1.72	0.026	1.007
3P,5	69.62	1.75	0.025	1.005
3P,6	74.1	1.86	0.025	1.0045
3P,7†	78.24	1.97	0.025	1.005
3P,8†	72.7	1.83	0.025	1.005
3P,9	77.78	1.96	0.025	1.006
3P,10	69.64	1.75	0.025	1.004

3P,11†	72.91	1.84	0.025	1.005
3P,12†	73.4	1.85	0.025	1.009
3P,13	74.74	1.88	0.025	1.008
3P,14	66.53	1.67	0.025	1.005
3P,15	77.15	1.94	0.025	1.0065
3P,16	67.77	1.7	0.025	1.006
3P,17	74.8	1.89	0.025	1.008
3P,18†	75.81	1.91	0.025	1.007
3P,19	74.66	1.88	0.025	1.005
3P,20*	60.65	1.52	0.025	1.005
3P,21†	67.72	1.77	0.026	1.004
3P,22†	66.71	1.68	0.025	1.007
3P,23	72.23	1.82	0.025	1.0075
3P,24	71.59	1.81	0.025	1.009
3P,25†	73.26	1.85	0.025	1.011
3P,26†	71.37	1.8	0.025	1.008
3P,27	66.19	1.74	0.026	1.009
3P,28†	69.38	1.75	0.025	1.007
3P,29	71.61	1.8	0.025	1.008
3P,30	65.61	1.65	0.025	1.005

† Specimen failed in delamination

*Data point not included in analysis because of defect in sample

Appendix B: Predicted Flexural Load of a 1-, 2-, and 3-ply tensile specimen

Predicted flexural loads for a sandwich panel with dimensions: $b = 3 \text{ in.}$, $h_c = 0.5 \text{ in.}$, $h = h_c + (2 * \text{ply thickness})$, $S = 22 \text{ in.}$, and $L = 4 \text{ in.}$.

Predicted Flexural Load		
1-Ply (lbs.)	2-Ply (lbs.)	3-Ply (lbs.)
74.89	209.11	306.89
83.08	188.49	313.67
78.24	209.80	300.89
76.10	199.67	285.85
77.95	194.56	290.96
82.74	199.83	309.69
70.35	203.88	326.99
71.67	207.99	303.83

71.19	195.61	325.07
96.49	184.74	291.05
84.10	205.69	304.71
85.72	201.02	306.76
71.03	211.96	312.36
80.90	204.90	278.05
76.19	177.62	322.43
57.00	179.89	283.23
55.58	176.74	312.61
60.98	180.52	316.83
62.48	171.83	312.03
50.30	182.21	253.47*
71.01	182.27	294.41
57.08	180.20	278.80
67.18	184.68	301.87
78.82	185.16	299.20
85.78	203.94	306.18
65.77	205.65	298.28
79.92	188.85	287.76
73.25	206.07	289.96
84.30	199.22	299.28
81.10	195.25	274.20
Average: 73.71	Average: 193.91	Average: 299.58

*Data point not included in analysis because of defect in sample